Microsc. Microanal., page 1 of 7
doi:10.1017/S1431927614013567

Microscopy AND Microanalysis

Validating Whole Slide Digital Morphometric Analysis as a Microscopy Tool

Robert B. Diller,[1] and Robert S. Kellar[1,2,*]

[1]*Department of Biological Sciences, Northern Arizona University, 617 S. Beaver St., P.O. Box 5640, Flagstaff, AZ 86011-5640, USA*
[2]*Development Engineering Sciences, LLC, 708 N. Fox Hill Rd, Flagstaff, AZ 86004, USA*

Abstract: Whole slide imaging (WSI) can be used to quantify multiple responses within tissue sections during histological analysis. Feature Analysis on Consecutive Tissue Sections (FACTS®) allows the investigator to perform digital morphometric analysis (DMA) within specified regions of interest (ROI) across multiple serial sections at faster rates when compared with manual morphometry methods. Using FACTS® in conjunction with WSI is a powerful analysis tool, which allows DMA to target specific ROI across multiple tissue sections stained for different biomarkers. DMA may serve as an appropriate alternative to classic, manual, histologic morphometric measures, which have historically relied on the selection of high-powered fields of views and manual scoring (e.g., a gold standard). In the current study, existing preserved samples were used to determine if DMA would provide similar results to manual counting methods. Rodent hearts ($n = 14$, left ventricles) were stained with Masson's trichrome, and reacted for cluster of differentiation 68 (CD-68). This study found no statistical significant difference between a classic, manual method and the use of digital algorithms to perform the similar counts ($p = 0.38$). DMA offers researchers the ability to accurately evaluate morphological characteristics in a reproducible fashion without investigator bias and with higher throughput.

Key words: digital pathology, digital analysis, digital morphometric analysis, whole slide analysis, whole slide quantitative analysis

Introduction

Whole slide imaging of glass microscope slides and the subsequent use of computer-aided quantitative analysis has been growing in popularity with use of digital imaging and its ability to create images with resolutions from 0.25 to 0.62 μm/pixel (Wang et al., 2007; Huisman et al., 2010; Lofgren et al., 2011). With standardization and long-term archiving of medical records, digital images will become an integral part of the electronic health record (Crowley et al., 2000). Current FDA-approved diagnostic applications of digital morphometric analysis (DMA) are widely and routinely used by drug pharmaceutical companies, such as in the realm of cancer tissue markers (Mulrane et al., 2008; Rocha et al., 2009; Daniel et al., 2011).

The advantages of using DMA has applications outside of pharmaceutical research and testing and can be adopted and customized for uses within basic or translational research. There are immediate, translatable benefits for the development and use of DMA: telepathology consultation, the use of technology for pathology consultation across great distances, and quantitative analysis of the entire tissue section in research applications in order to provide a quantitative component to diagnostic pathology (Potts et al., 2010; Hipp et al., 2011; Nassar et al., 2011; Al-Janabi et al., 2012). Performing DMA across an entire slide provides the investigator with a semi-automated, reproducible method to evaluate histology more quickly with higher throughput capabilities (Feldman, 2008; López et al., 2008; Klapczynski et al., 2011; Nassar et al., 2011). DMA reduces analysis time, generates quantitative data, and allows for reproducibility because the exact parameters and assumptions can be used across every sample in a particular study with no inter-investigator bias (Feldman, 2008; López et al., 2008; Słodkowska et al., 2010; Klapczynski et al., 2011; Nassar et al., 2011; Webster & Dunstan, 2014).

In the current study, DMA was performed to demonstrate that quantitative computational analysis and digital morphometric counts can be used as a reliable morphometric tool compared with classical manual counting methods. For this comparison, manually stained samples were selected because they contain inherent variability and differences in positive staining and non-specific background staining. This was important for the current comparison considering that many automated analytical tools have difficulty in discriminating subtleties that the human eye can detect. In this fashion, the current morphological comparisons (e.g., DMA versus manual methods) may be considered a rigorous and conservative approach where manual methods may be thought to be superior to automated methods due to inherent sample variability. Therefore, manual staining methods were selected to demonstrate the successful use of DMA on a wide range and variety of manually or auto-stained slides (Weinstein et al., 2009; Potts et al., 2010). Two automated morphology tools were used, Feature Analysis on Consecutive Tissue Sections (FACTS®) and DMA, to compare against two

Received May 27, 2014; accepted October 23, 2014
*Corresponding author. rskellar@des-company.com

human investigators using traditional manual counting methods (Potts et al., 2011).

Materials and Methods

Slide Scanner

All glass slides were digitally scanned using the Aperio CS slide scanner using a 20× Olympus objective. At 20× magnification, the Aperio scanner provides a digital image with a resolution of 0.5 μm/pixel (Aperio, Vista, CA, USA).

Tissue used for Morphometric Assessment and Histology

Samples of infarcted left ventricular tissue ($n = 14$) from a male Sprague–Dawley rat model were formalin fixed and paraffin embedded. The tissues were sectioned at 6 μm and subsequently processed for staining and immunohistochemistry. In order to determine the specific area of infarct, the tissues were stained with Masson's trichrome. The infarct was identified by the large collagen deposition, which stains a distinct bright blue (Saraswati et al., 2010; Segura et al., 2011). Serial sections were also reacted with cluster of differentiation 68 (CD-68; Serotec, clone ED1, Raleigh, NC, USA) used at a final dilution of 1:100. The primary antibody was visualized using a secondary antibody with a peroxidase reaction product recognition system (Universal mouse kit; Dako Inc., Carpinteria, CA, USA). Tissues were then counterstained with methyl green to identify background nuclei (Kellar et al., 2011). CD-68 is a protein that is expressed in the cytoplasm of activated macrophages and was selected for this analysis because of the high specificity of the antibody in damaged myocardium and the resulting punctate cytoplasmic staining pattern (Doussis et al., 1993; Kellar et al., 2011). This provides a distinct and clear positive signal for both DMA and human investigator evaluation. All staining and immunohistochemistry reactions were performed by hand, which created tissues with varying degrees of background staining.

Annotations (Digital Image Mark-Up)

For this validation study, FACTS® was used to ensure all measurements occurred specifically within the area of infarct. FACTS® is a commercial algorithm developed by Flagship Biosciences (Westminster, CO, USA) histological and image analysis processes that allows quantitative multiplexing of histopathology tests (Potts et al., 2011). Using a reference slide to determine specific areas of interest, a region of interest (ROI) was created and transferred across semi-serial slides that were stained to determine specific histological features. Each slide contained two sections of the ventricles; therefore, sections on each slide were not exact serial sections, but were ~10 μm apart. This allowed the analysis to be performed within the specified ROI on each subsequent slide, in this case specifically in the area of scarring within the infarct of the myocardium. FACTS® has the ability to change angles and size. It is nearly impossible to mount a tissue section in exactly the same conformation when creating serial or semi-serial slides.

The scarred myocardial tissue was encircled using an inclusion pen marker to identify the ROI. This annotation was transferred across to the target slides. In this case, the annotations were transferred to samples reacted with CD-68. Once the area to be analyzed was correctly transferred to the CD-68-reacted serial section of the infarcted tissue, a grid map was placed inside the annotated area (Fig. 1).

This grid program allowed the user to specify the size of the grids used. The program placed a grid map into the specified area of inclusion. For this study, a grid of 100 × 100 pixels was used, which is 400.2 μm^2. Next, a random number generator was used to identify ten random grid boxes (400.2 μm^2) for analysis. Once the grid boxes were identified, they were numbered one through ten. The counts were performed only within these ten identified grids. In order for a specified grid to be used for counts it must have met the following requirements: all four corners of the grid had to be in contact with tissue and no folds or other tissue artifacts could be within the grid space. If a randomly chosen grid did not meet the criteria a new grid was chosen at random.

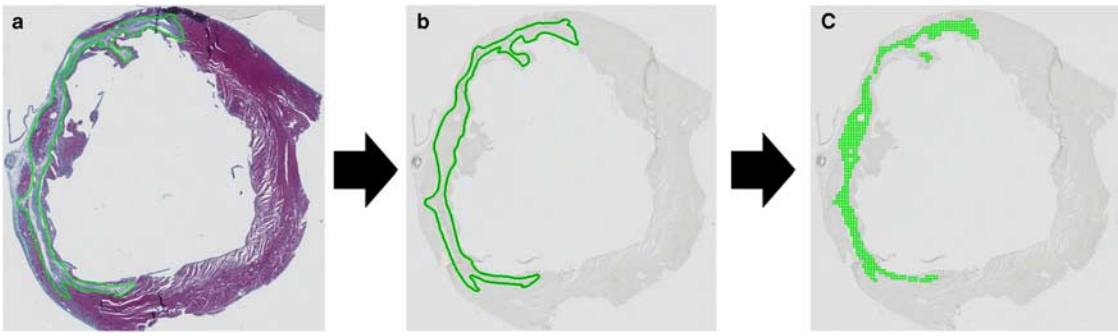

Figure 1. Illustration of the Feature Analysis on Consecutive Tissue Sections (FACTS®) process being used across tissue sections. **a:** The trichrome stained slide was used to accurately determine the area of the infarct within the rodent left ventricle. **b:** The specific infarct area was transposed onto a cluster of differentiation 68 (CD-68) reacted heart. **c:** The grid was placed within the area determined by the trichrome stained section.

Nuclear counting algorithm V9 (Aperio) was then used to analyze the same grids.

Human Investigator Counts

Two investigators independently performed counts of CD-68$^+$ stained macrophages in each of the ten grids identified. All fragments and whole cells, positive for CD-68 IHC were counted. This was a required inclusion criteria as this antibody has high specificity to activated tissue macrophages. The count data was reported as counts per grid: the number of active macrophages present in a 400.2 μm^2 area.

Digital Algorithm

Nuclear Image Analysis v9 (Aperio; Fig. 2) is a cellular counting algorithm, which uses input factors based on cellular profiles. CD-68$^+$ cell parameters were defined by adjusting digital values including nuclear size, roundness, compactness, and elongation. These parameters are adjustable to assist the user with determining the appropriate amount of cellular segmentation. The user can adjust the color values based on the staining of interest. For example, the user can use an "eye dropper" tool, which allows the user to choose specific colors and gradients of color to use as the "positive stain" being measured and the background stain. The "eye dropper" tool then provides the user with a break-down of the color into its red, blue, and green components. In the algorithm set-up, the user can also change the threshold method in order to determine how the algorithm identifies the edges of the cell. This uses the colors that the user inputs and changes the way the algorithm segments the cell. There is an "amplitude threshold", which adjusts according to the mean intensity of all the pixels and automatically thresholds to one sigma above the mean. The edge threshold method automatically adjusts the threshold according to the mean of edge pixels; it uses an edge finding method to identify the edge pixels and averages these values to determine the threshold. The manual threshold method uses an upper and lower limit set by the user to eliminate any unwanted background, but it will not automatically adjust to compensate for any lighter or darker staining between slides. The current study used the edge threshold method. The algorithm was adjusted using the parameters identified in the Aperio user's guide (http://tmalab.jhmi.edu/aperiou/userguides/IHC_Nuclear.pdf).

Statistical Analysis

An analysis of variance (ANOVA) was performed with a Tukey's HSD *post hoc* using JMP Pro 10 (SAS, Cary, NC, USA). Statistical significance was set at $p < 0.05$.

Results

The average number of CD-68$^+$ cells in 14 unique infarcted myocardium samples from a rodent model were counted by each human investigator and the DMA (see Fig. 3 for a comparison of the counts on one of the samples and see Fig. 4 for a graphical representation of all 14 samples). These data demonstrate that all three analytical methods (the two investigators and the computational algorithm) resulted in similar values from ten fields of view from each sample. No statistical difference was seen using an ANOVA statistical comparison ($n = 14$; $p = 0.38$).

Discussion

Traditionally, manual cell counting has been performed to analyze histological specimens and currently represents the gold standard (Jara-Lazaro et al., 2010). Significant technological advances are now available for the analysis of histological specimens that may be less accurate than manual methods, but may afford advantages for the researcher. These advances may help to improve and maximize effectiveness of whole slide analysis while allowing for higher throughput during analysis for larger studies (see Table 1). The use of DMA has the same effectiveness as historical manual methods while also providing the researcher a more objective analysis by removing subjectivity through the elimination of inter-investigator biases.

In analysis of pathology samples, manual methods represent the central dogma, which includes use of photomicrographs of a selected number of high-powered fields of view and performing visual or digital measurements across these images (Kidd et al., 2001; Cole et al., 2007; Fujimoto et al., 2007). These manual methods can introduce bias

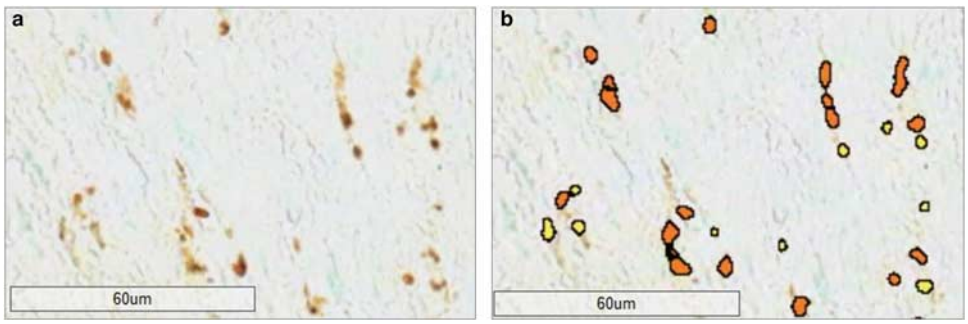

Figure 2. Representative image of the nuclear counting algorithm. **a:** Histological section reacted with cluster of differentiation 68 (CD-68) to be analyzed. **b:** Representative image with the false color mark-up of the same section identified as **a**. Yellow = low intensity, Orange = moderate intensity. Scale bar is 60 μm.

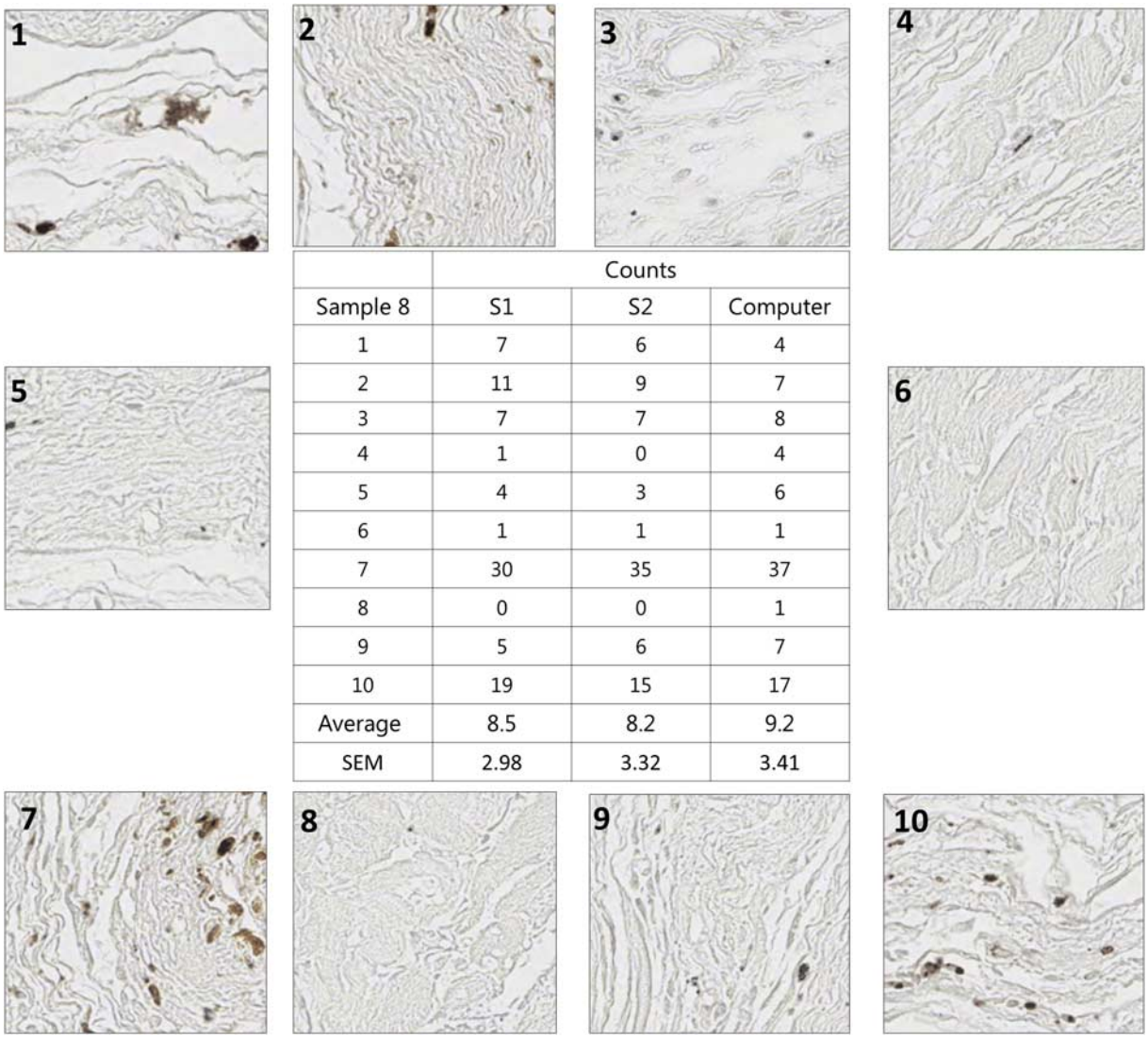

	Counts		
Sample 8	S1	S2	Computer
1	7	6	4
2	11	9	7
3	7	7	8
4	1	0	4
5	4	3	6
6	1	1	1
7	30	35	37
8	0	0	1
9	5	6	7
10	19	15	17
Average	8.5	8.2	9.2
SEM	2.98	3.32	3.41

Figure 3. Representative images of the ten random fields identified on Sample no. 8 reacted with cluster of differentiation 68 (CD-68). The table contains the counts of each of the investigators as well as the digital morphometric analysis (DMA) counts.

within the data analysis because the investigator may be unintentionally drawn to areas (or focus on areas) that have a high concentration of stain (or are absent of stain) within high-powered fields of view (Hsu et al., 2003; Evans et al., 2008; Nasser et al., 2011). Therefore, the true morphometric result of the staining within a sample may not be analyzed, and instead only a narrow area may be evaluated and reported as representative of the sample.

In this study, we report the results of a narrow area of the tissue sample being analyzed (ten random fields of view) using two different methods: a classic manual counting method was compared with DMA. This comparison was performed to validate that digital morphometry methods can deliver results similar to well-accepted manual counting methods. Most studies have numerous design parameters that are equally as important as accurate counting. For example, consistency in analysis can vary during manual methods when evaluations are performed over extended periods of time or by multiple investigators. Investigators may perform manual evaluations over extended periods of time when data collection is at discrete long-term time-points, or in larger studies the manual analysis may extend for days, weeks, or months. Furthermore, inter-investigator bias can significantly impact the consistency of data analysis. With manual methods it is common for more than one investigator to perform measurements and counts. Additional precautions and planning can be taken to average out any differences between the investigators; however, in many labs the individual researchers and staff can change. Depending on how these individuals were trained, they may each interpret the histology, positive stain, or morphology characteristics differently. Computational whole slide analysis removes these biases by performing consistent measurements with the same initial design inputs across all samples being analyzed from

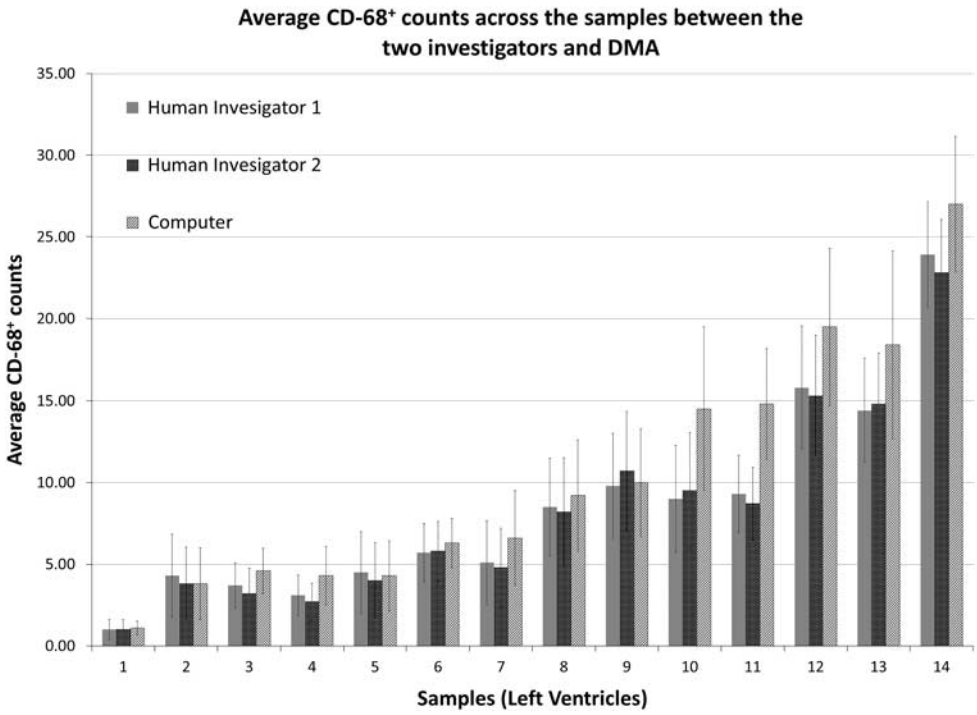

Figure 4. Graphical representation comparing the counts of cluster of differentiation 68 (CD-68) activated macrophages between two scientists and the nuclear counting algorithm (computer) across ten fields of view within the area of infarct within the left ventricle of a rodent.

Table 1. Representative Table of the Amount of Time in Hours Required to Perform Analysis Both Manually and using DMA, Given the Mentioned Assumptions.

	Manual Methods			DMA			
Number of Slides in Study	Investigator no. 1 (10 Fields of View)	Investigator no. 2 (10 Fields of View)	Total Analysis Time	Whole Slide Scanning	Algorithm Calibration[a]	DMA	Total Analysis Time
100.0	16.7	16.7	33.3	3.3	1.0	3.3	7.7
500.0	83.3	83.3	166.6	16.7	1.0	16.7	34.3
1000.0	166.7	166.7	333.3	33.3	1.0	33.3	67.7
5000.0	833.3	833.3	1666.7	166.7	1.0	166.7	334.3
10000.0	1666.7	1666.7	3333.3	333.3	1.0	333.3	667.7

It is evident that there is a great deal of time saved even in a smaller 100 slide study between the two methods.
Assumptions: staining methods whether manual or automated result in similar amount of processing time. Manual, Investigators conduct morphometry analysis in a blinded fashion. Manual, 1 field of view = 1 min of morphometry counting, analysis and statistics. DMA, whole slide scanning = 2 min per slide with a 20× objective using Aperio Scan Scope XT (120 slide cartridge). DMA, quad core processor = 2 min per slide. DMA, entire slide analyzed rather than only ten fields of view.
[a]Algorithm calibration can typically be reduced if the tissue staining is consistent e.g. by employing automated staining and if the calibration is being performed by experienced imaging scientists.
DMA, digital morphometric analysis.

one study to another, even over extended periods of time. A significant advantage of performing DMA is that the investigator receives a more comprehensive overview of the whole tissue sample being analyzed versus traditional manual methods that are currently used. The analysis can be performed across the entire sample rather than only focusing on a specific number of fields of view; therefore, providing better feedback to the investigator about the sample as the ROI. In this study, we focused on specific fields of view, to validate the results to well accepted manual methods. However, in our lab we now routinely use whole slide digital analysis for our morphometry evaluations.

In the current study, we demonstrate that digital algorithms can be used as an appropriate alternative to traditional manual methods. These novel methods can be valuable in studies with large sample sizes, multiple stains of

IHC, long-term or multiple time points of data collection, large sample archival needs, fluorescent immunohistochemistry that can fade over time (digital scanning preserves the original signal), and when numerous or new researchers are analyzing histological results.

Conclusions

DMA gives investigators a novel measurement tool to evaluate histological features and characteristics that are highlighted microscopically. The use of digital analysis has been well described in pharmacological drug discovery markets for several years without yet being widely adopted into the research or academic communities who conduct basic or translational research and routinely use histomorphometry as an outcome measure of their experiments. The validation of this algorithm should provide a basis for continued research and exploration on how to better leverage digital, high throughput techniques to improve research outcomes.

Acknowledgments

The authors thank Flagship Biosciences for the use of their Aperio scanners and algorithms.

References

Al-Janabi, S., Huisman, A. & Van Diest, P.J. (2012). Digital pathology: Currents status and future perspectives. *Histopathology* **61**, 1–9.

Cole, B., Gomoll, A., Yanke, A., Pylawka, T., Lewis, P., MacGillivray, J. & Williams, J. (2007). Biocompatibility of a polymer patch for rotator cuff repair. *Knee Surg Sports Traumatol Arthrosc* **15**(5), 632–637.

Crowley, R.S., Gadd, C.S., Naus, G., Becich, M. & Lowe, H.J. (2000). Defining the role of anatomic pathology images in the multimedia electronic medical record—a preliminary report. *Proc AMIA Symp*, 161–165.

Daniel, C., Rojo, M.G., Klossa, J., Mea, V.D., Booker, D., Beckwith, B.A. & Schrader, T. (2011). Standardizing the use of whole slide images in digital pathology. *Comput Med Imaging Graph* **35** (7–8), 496–505.

Doussis, I.A., Gatter, K.C. & Mason, D.Y. (1993). CD68 reactivity of non-macrophage derived tumours in cytological specimens. *Journal of clinical pathology* **46**(4), 334–336.

Evans, A.J., Henry, P.C., Van der Kwast, T.H., Tkachuk, D.C., Watson, K., Lockwood, G.A. & Srigley, J.R. (2008). Interobserver variability between expert urologic pathologists for extraprostatic extension and surgical margin status in radical prostatectomy specimens. *Am J Surg Pathol* **32**(10), 1503–1512.

Feldman, M.D. (2008). Beyond morphology: Whole slide imaging, computer-aided detection, and other techniques. *Arch Pathol Lab Med* **132**(5), 758–763.

Fujimoto, K.L., Tobita, K., Merryman, W.D., Guan, J., Momoi, N., Stolz, D.B. & Wagner, W.R. (2007). An elastic, biodegradable cardiac patch induces contractile smooth muscle and improves cardiac remodeling and function in subacute myocardial infarction. *J Am Coll Cardiol* **49**(23), 2292–2300.

Hipp, J., Flotte, T., Monaco, J., Cheng, J., Madabhushi, A., Yagi, Y., Rodriguez-Canales, J., Emmert-Buck, M., Dugan, M., Hewitt, S., Toner, M., Tompkins, R., Lucas, D., Gilbertson, J. & Balis, U. (2011). Computer aided diagnostic tools aim to empower rather than replace pathologists: Lessons learned from computational chess. *J Pathol Inform* **2**, 25.

Hsu, C.Y., Ho, D.M.T., Yang, C.F. & Chiang, H. (2003). Interobserver reproducibility of MIB-1 labeling index in astrocytic tumors using different counting methods. *Mod Pathol* **16**(9), 951–957.

Huisman, A., Looijen, A., van den Brink, S.M. & van Diest, P.J. (2010). Creation of a fully digital pathology slide archive by high-volume tissue slide scanning. *Hum Pathol* **41**(5), 751–757.

Jara-Lazaro, A.R., Thamboo, T.P., Teh, M. & Tan, P.H. (2010). Digital pathology: Exploring its applications in diagnostic surgical pathology practice. *Pathology* **42**(6), 512–518.

Kellar, R.S., Lancaster, J.J., Thai, H.M., Juneman, E., Johnson, N.M., Byrne, H.G., Stansifer, M., Arsanjani, R., Baer, M., Bebbington, C., Flashner, M., Yarranton, G. & Goldman, S. (2011). Antibody to granulocyte macrophage colony-stimulating factor reduces the number of activated tissue macrophages and improves left ventricular function after myocardial infarction in a rat coronary artery ligation model. *Journal of cardiovascular pharmacology* **57**(5), 568–574.

Kidd, K.R., Dal Ponte, D.B., Kellar, R.S. & Williams, S.K. (2001). A comparative evaluation of the tissue responses associated with polymeric implants in the rat and mouse. *J Biomed Mater Res* **59**(4), 682–689.

Klapczynski, M., Gagne, G.D., Morgan, S.J., Larson, K.J., LeRoy, B.E., Blomme, E.A. & Shek, E.W. (2011). Computer-assisted imaging algorithms facilitate histomorphometric quantification of kidney damage in rodent renal failure models. *J Pathol Inform* **3**, 20.

Lofgren, K.A., Ostrander, J.H., Housa, D., Hubbard, G.K., Locatelli, A., Bliss, R.L. & Lange, C.A. (2011). Mammary gland specific expression of Brk/PTK6 promotes delayed involution and tumor formation associated with activation of p38 MAPK. *Breast Cancer Res* **13**(5), R89.

López, C., Lejeune, M., Salvadó, M.T., Escrivà, P., Bosch, R., Pons, L.E. & Jaén, J. (2008). Automated quantification of nuclear immunohistochemical markers with different complexity. *Histochem Cell Biol* **129**(3), 379–387.

Mulrane, L., Rexhepaj, E., Penney, S., Callanan, J.J. & Gallagher, W.M. (2008). Automated image analysis in histopathology: a valuable tool in medical diagnostics. *Expert Reviews of Molecular Diagostics* 8.6: 707.

Nassar, A., Cohen, C., Albitar, M., Agersborg, S.S., Zhou, W., Lynch, K.A. & Siddiqui, M.T. (2011). Reading immunohistochemical slides on a computer monitor—a multisite performance study using 180 HER2-stained breast carcinomas. *Appl Immunohistochem Mol Morphol* **19**(3), 212–217.

Potts, S.J., Johnson, T.D., Voelker, F.A., Lange, H. & Young, G.D. (2011). Multiplexed measurement of proteins in tissue in a clinical environment. *Appl Immunohistochem Mol Morphol* **19**(6), 494–498.

Potts, S.J., Young, G.D. & Voelker, F.A. (2010). The role and impact of quantitative discovery pathology. *Drug Discov Today* **15**(21–22), 943–950.

Rocha, R., Vassallo, J., Soares, F., Miller, K. & Gobbi, H. (2009). Digital slides: Present status of a tool for consultation, teaching, and quality control in pathology. *Pathol Res Pract* **205**(11), 735–741.

Saraswati, S., Alfaro, M.P., Thorne, C.A., Atkinson, J., Lee, E., & Young, P.P. (2010). Pyrvinium, a potent small molecule Wnt inhibitor, promotes wound repair and post-MI cardiac remodeling. *PLoS One* **5**(11), e15521.

Segura, A.M., Frazier, O.H., Demirozu, Z. & Buja, L.M. (2011). Histopathologic correlates of myocardial improvement in patients supported by a left ventricular assist device. *Cardiovascular Pathology* **20**(3), 139–145.

Słodkowska, J., Filas, V., Buszkiewicz, E., Trzeciak, P., Wojciechowski, M., Koktysz, R. & Garcia Rojo, M. (2010). Study on breast carcinoma Her2/neu and hormonal receptors status assessed by automated images analysis systems: ACIS III (Dako) and ScanScope (Aperio). *Folia Histochem Cytobiol* **48**(1), 19–25.

Wang, Y., Turner, R., Crookes, D., Diamond, J. & Hamilton, P. (2007). Investigation of methodologies for the segmentation of squamous epithelium from cervical histological virtual slides. In *Machine Vision and Image Processing Conference, 2007 IMVIP 2007*, pp. 83–90. IEEE, NUI Maynooth, Ireland.

Webster, J.D. & Dunstan, R.W. (2014). Whole-slide imaging and automated image analysis considerations and opportunities in the practice of pathology. *Vet Pathol Online* **51**(1), 211–223.

Weinstein, R.S., Graham, A.R., Richter, L.C., Barker, G.P., Krupinski, E.A., Lopez, A.M. & Gilbertson, J.R. (2009). Overview of telepathology, virtual microscopy, and whole slide imaging: Prospects for the future. *Hum Pathol* **40**(8), 1057–1069.